

# GEOMETRIC FLOWS AND SPACE-PERIODIC SOLITONS ON THE LIGHT-CONE

YUN YANG\*

**ABSTRACT.** This paper investigates curve flows on the light-cone in the 3-dimensional Minkowski space. We derive the Harnack inequality for the heat flow and present a detailed classification of space-periodic solitons for a third-order curvature flow. The nontrivial periodic solutions to this flow are expressed in terms of the Jacobi elliptic sine function. Additionally, the closed soliton solutions form a family of transcendental curves, denoted by  $x_{p,q}$ , which are characterized by a rotation index  $p$  and close after  $q$  periods of their curvature functions. The ratio  $p/q$  satisfies  $p/q \in (\sqrt{2/3}, 1)$ , where  $p$  and  $q$  are relatively prime positive integers. Guided by the classification process, we obtain the analytic solutions to a second-order nonlinear ordinary differential equation.

## 1. INTRODUCTION

The light-cone represents the boundary in which information can travel, with the speed of light serving as the ultimate limit, and the idea arises directly from Einstein's theory of special relativity [Einstein 1905], which states that the speed of light is constant for all observers, regardless of their motion. Originating from a specific event at its vertex, the light-cone divides space-time into future and past cones, illustrating the spatial and causal relationships between events [Misner et al. 1973, Nakahara 2003]. In mathematics, Lorentzian manifolds [Minkowski 1908, Vranceanu and Roşca 1976] provide a framework for modeling curved space-time, with the light-cone characterized using semi-Riemannian geometry to examine the metric and curvature properties of space-time [O'Neill 1983, Sachs and Wu 1977]. In fact, the light-cone is a pivotal instrument in comprehending degenerate geometry of space-time manifolds [Duggal and Bejancu 1996]. It can be envisioned as the light-speed hyperplane at a particular space-time point, profoundly influencing the overall metric structure of space-time. Furthermore, it serves as the foundation for defining geodesics [Benci and Fortunato 1994], which delineate the paths along which particles traverse the shortest conceivable routes within a given space-time geometry. Additionally, the light-cone is intricately linked to gravitational fields and the curvature of space-time, as elucidated by Einstein's field equations [Parikh and Svesko 2018].

---

\* Corresponding author: yangyun@mail.neu.edu.cn

2020 *Mathematics Subject Classification.* 53A35, 53E40, 35Q51, 34A05.

*Key words and phrases.* light-cone; soliton; curvature flow; Killing vector field.

In physics, the light-cone casts a long shadow, defining the ultimate velocity of information dissemination—the speed of light, a cornerstone of special relativity [Rindler 2001]. Through the mathematical framework of light-cones, Hawking and Ellis systematically explores causal structures, singularities, black holes, and cosmology [Hawking and Ellis 1973]. The light-cone has been instrumental in proving singularity theorems, analyzing black hole horizons, and gaining insights into the universe’s expansion and structure [Hawking 1965, Hawking 1966a, Hawking 1966b, Hawking 1967, Penrose 1965, Penrose 2020].

Periodic solutions represent a vital mathematical tool in describing periodic phenomena and unraveling the behavior of nonlinear systems. In mathematical physics, the study of periodic solutions not only elucidates periodic occurrences in nature but also lays the theoretical groundwork for comprehending nonlinear physical systems [Birkhoff 1927, Kovalev 2015, Poincaré 1892]. These solutions are ubiquitous in fields like mechanics, vibration theory, optics, electromagnetism, chaos, and bifurcations (for more details see [Strogatz 1994]). While exact solutions for numerous physical systems remain elusive, periodic solutions can be procured through numerical methods or approximations, thereby aiding in the anticipation of system behavior and guiding experimental endeavors [Press et al. 2007].

Geometric flows are generally described by partial differential equations that govern the evolution of geometric structures, such as surfaces, manifolds, or other geometric objects (for more details refer to [Brakke 1978, Evans and Spruck 1991, Hamilton 1982, Olver 2008]). These equations define how the geometric object evolves over time, shaping its properties in response to the flow. A key concept in the study of geometric flows is that of soliton solutions, which arise from nonlinear partial differential equations. Solitons are stable solutions, particularly in the context of wave propagation. A distinctive property of solitons is that they maintain their shape during propagation [Gardner et al. 1967, Zabusky and Kruskal 1965]. This feature has found analogous applications in geometric flows, where solitons often serve as steady solutions that reflect the stability of certain geometric structures under the flow (refer to [Andrews and Baker 2004, Hungerbuhler and Smoczyk 2000, Perelman 2002]). In the study of geometric flows, one of the most crucial challenges is understanding the nature of singularities. These singularities are intimately connected to the topological structure of the manifold. Investigating them is essential for gaining a deeper understanding of the manifold’s geometric and topological properties. Moreover, such investigations are critical for revealing the manifold’s multifaceted behavior. Soliton solutions play a significant role in this context, as they provide a prototypical framework for both the emergence and resolution of singularities in geometric flows (see [Huiskens 1990, Huiskens 1993] for further details).

In this paper, we primarily focus on the curve flow occurring on the right half of a light-cone, denoted as  $LC^*$ , which can be expressed in spherical

coordinates as  $(\psi, \psi \cos \theta, \psi \sin \theta)$  subject to the constraint  $\psi > 0$ . Let  $\mathbf{r}_0$  represent a curve situated on  $LC^*$ . We then consider the motion of curves on  $LC^*$  characterized as

$$\frac{\partial \mathbf{r}}{\partial t} = U\mathbf{r} + W\mathbf{T}, \quad \mathbf{r}(\cdot, 0) = \mathbf{r}_0, \quad (1.1)$$

where  $\mathbf{T}$  denotes the unit tangent vector field. Notably,  $U$  and  $W$  remain invariant under Lorentz transformations in the Minkowski space  $\mathbb{E}_1^3$ . In Section 3, we demonstrate that this flow guarantees that the motion of the curves will consistently remain confined to  $LC^*$ .

This flow induces the evolutionary equations for the following quantities

$$\frac{g_t}{g} = U + W_s,$$

and

$$(k_g)_t = U_{ss} - 2k_g U + W(k_g)_s,$$

where  $g$  is the metric of curve  $\mathbf{r}$ , which depends on the pseudo-scalar product introduced in Section 2. Here,  $s$  denotes the corresponding arc length parameter, and  $k_g$  signifies the curvature of the curve  $\mathbf{r}$  on  $LC^*$  as defined in (2.5).

Geometric heat flow [Hamilton 1989] refers to the evolution of a family of submanifolds  $F : M \times (0, T) \rightarrow N$  that satisfies the partial differential equation

$$\frac{\partial}{\partial t} F = \Delta F,$$

where  $F(\cdot, 0) = F_0 : M \rightarrow N$  represents the initial condition. Here,  $\Delta$  denotes the Laplace-Beltrami operator on  $(M, g)$ , with  $g$  being the metric on the manifold  $M$ . The curve shortening flow (CSF) is one of the simplest and well-studied models [Gage 1983, Gage 1984, Gage and Hamilton 1986]. The higher dimensional analogue of CSF is the mean curvature flow (MCF) [Brakke 1978, Colding and Minicozzi 2003, Huisken 1990]. The Ricci flow (RF) [Hamilton 1982, Hamilton 1995b] deforms an initial metric in the direction of its Ricci tensor, and shares many similarities with CSF and MCF. All these flows are collectively referred to as geometric heat flows. There are some analogical extensions of the geometric heat flow in affine geometry [Angenent et al. 1998, Olver et al. 2020, Sapiro and Tannenbaum 1994, Yang 2023].

When we choose  $U = k_g$  and  $W = 0$ , the flow given by equation (1.1) simplifies to the heat flow, which is expressed as

$$\frac{\partial \mathbf{r}}{\partial t} = k_g \mathbf{r}. \quad (1.2)$$

Consequently, the evolutionary equations undergo a modification, becoming  $\frac{g_t}{g} = k_g$  and  $(k_g)_t = (k_g)_{ss} - 2k_g^2$ . To gain further insight into this flow, consider the following illustrative example.

**Example 1.1.** The curves defined by

$$\mathbf{r} = (\sqrt{-t}, \sqrt{-t} \cos \theta, \sqrt{-t} \sin \theta),$$

evolve according to the heat flow. During this evolution, we have

$$k_g = \frac{1}{2t},$$

where time  $t$  ranges in  $(-\infty, 0)$ .

In [Silva and Tenenblat 2023], several classification results for solitons of this heat flow on the light-cone have been obtained.

The Li-Yau Harnack inequality, introduced in [Li and Yau 1986], serves as a potent instrument in the study of geometric flows. It offers profound insights into various aspects of these flows, including the behavior of solutions, their regularity, the formation of singularities, and the long-term convergence of the flow dynamics. This inequality has found widespread application in analyzing Ricci flow, mean curvature flow, and numerous other geometric flows, as demonstrated in [Andrews 1994, Bryan et al. 2020, Chow 1991, Hamilton 1993, Hamilton 1995a]. By taking the notation  $k = -k_g$ , we derive a Harnack inequality specific to the heat flow on the light-cone  $LC^*$  (see Section 3.1 for the proof).

**Theorem 1.2** (Harnack Inequality). *For an immersed solution to the curve flow (1.2) on the light-cone  $LC^*$  with  $k > 0$  and defined on the time interval  $[t_0, T)$ , we have the following Harnack inequality*

$$k_t - \frac{k_s^2}{k} - k^2 + \frac{k}{2(t - t_0)} \geq 0.$$

Another noteworthy flow arises when we set  $U = (k_g)_s$  and  $W = -k_g$ , that is,

$$\frac{\partial \mathbf{r}}{\partial t} = (k_g)_s \mathbf{r} - k_g \mathbf{T}, \quad (1.3)$$

leading to the evolutionary equations

$$g_t = 0, \quad (k_g)_t = (k_g)_{sss} - 3k_g(k_g)_s.$$

These equations embody a KdV (Korteweg-de Vries) equation, a renowned nonlinear partial differential equation that is extensively utilized to model wave behaviors across various physical scenarios. In this specific flow, the condition  $g_t = 0$  signifies that the flow exhibits non-stretching characteristics. Consequently, we denominate this flow as the third-order centro-affine curvature flow.

In fact, when both  $g_t = 0$  and  $(k_g)_t = 0$  are satisfied, it signifies that the curves retain their original shapes throughout the evolutionary process driven by the flow defined in (1.1). Hence, these curves constitute a distinctive category of solitons for the flow. Through integration, we obtain

$$(k_g)_{ss} - \frac{3}{2}k_g^2 + \frac{\lambda}{2} = 0, \quad ((k_g)_s)^2 - k_g^3 + \lambda k_g + \mu = 0, \quad (1.4)$$

where  $\lambda$  and  $\mu$  are the integration constants. Our primary focus is on studying nontrivial periodic soliton solutions. Notably, nontrivial periodic solutions to (1.4) may exist only when  $\lambda > 3(\mu/2)^{2/3}$ . In this case, the cubic equation  $x^3 - \lambda x - \mu = 0$  have three distinct real root, which we denote as  $x_1 < x_2 < x_3$ . Furthermore, the periodic solutions for (1.4) can be expressed in terms of the Jacobi sine function

$$k_g = x_1 + (x_2 - x_1)\text{sn}^2\left(\frac{\sqrt{x_3 - x_1}}{2}s, \sqrt{\frac{x_2 - x_1}{x_3 - x_1}}\right),$$

and the task to identify the periodic solitons is equivalent to solving the equation

$$\psi_{ss} - \frac{\psi_s^2 + 1}{2\psi} - \left(x_1 + (x_2 - x_1)\text{sn}^2\left(\frac{\sqrt{x_3 - x_1}}{2}s, \sqrt{\frac{x_2 - x_1}{x_3 - x_1}}\right)\right)\psi = 0. \quad (1.5)$$

For more detailed information, refer to Section 4. Equation (1.5) represents a complex second-order ordinary differential equation, and typically, finding its analytical solutions is a challenging task. However, during our endeavor to classify periodic soliton solutions, we have been fortunate to uncover some analytical solutions to this equation.

In the Minkowski space  $\mathbb{E}_1^3$ , periodic curves can be created by rotating the points in the initial period around axes that can be either space-like, time-like, or light-like. Our analysis of the periodic solitons related to (1.4) shows that the nature of their rotation hinges on the value of  $\mu$ . Specifically,

- When  $\mu > 0$ , the periodic solitons rotate around time-like axis.
- When  $\mu = 0$ , the periodic solitons rotate around light-like axis.
- When  $\mu < 0$ , the periodic solitons rotate around space-like axis.

Importantly, only when  $\mu > 0$  can closed solitons be formed .

For  $\mu > 0$ , an appropriate rotation can align the rotation axis with the  $x$ -axis, allowing us to derive one solution to (1.5) as

$$\psi = \frac{-k_g}{\sqrt{\mu}}.$$

Assuming the starting point is at  $\theta = 0$ , at the endpoint of the initial period, the progression angle  $\theta(T, \lambda)$  monotonically increases from  $2\sqrt{2/3}\pi$  to  $2\pi$  as  $\lambda$  varies from  $3(\mu/2)^{2/3}$  to  $+\infty$ . Here  $T$  denotes the period and is dependent on  $\lambda$ .

Abresch and Langer [Abresch and Langer 1986] studied the closed soliton solutions of normalized curve shortening flow by adding a tangential field to maintain constant speed along the curve in Euclidean plane. Analogously, Lopez De Lima and Montenegro [Lima and Montenegro 1999] renormalized the flow by adjusting the tangent component to preserve constant affine speed. Notably, in [Abresch and Langer 1986, Lima and Montenegro 1999], the rational number  $q/p$  was confined to the open interval  $(1/2, \sqrt{2}/2)$ . In the context of curve flow in centro-affine geometry, explored further in

[Jiang et al. 2023, Olver et al. 2020, Yang 2023], the rational ratio  $q/p$  expands its scope to encompass the union of two open intervals  $(0, 1/2) \cup (1/2, +\infty)$  [Niu and Yang 2025]. Transitioning to the focus of this paper, which examines solitons on the light-cone, we find that the rational ratio  $q/p$  resides in the specific open interval  $(\sqrt{2/3}, 1)$  (refer to Section 4.1 for more details).

**Theorem 1.3.** *Let  $\mathbf{x}$  be a closed solitons for the flow (1.3) on the light-cone. Then we have the following possibilities for  $\mathbf{x}$ :*

- (1)  $\mathbf{x}$  is a planar ellipse;
- (2)  $\mathbf{x} = \mathbf{x}_{p,q}$  has rotation index  $p$  and closes up in  $q$  periods of its curvature function. The pair  $(p, q)$  is not arbitrary and must be such that  $p/q$  is defined in the open interval  $(\sqrt{2/3}, 1)$ .

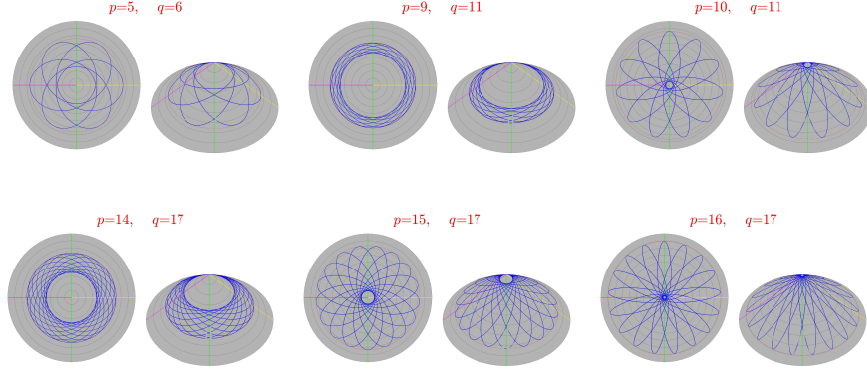


FIGURE 1. The closed solitons on light-cone.

In Fig. 1, several examples of closed solitons are presented. These closed curves exhibit a circular motion up and down within the range  $\frac{-x_2}{\sqrt{\mu}} \leq \psi \leq \frac{-x_1}{\sqrt{\mu}}$ . The illustration demonstrates that as  $p/q$  approaches  $\sqrt{2/3}$ , the difference  $x_2 - x_1$  tends to 0. Conversely, as  $p/q$  approaches 1, the difference  $x_2 - x_1$  tends to  $+\infty$ .

For  $\mu = 0$ , an appropriate rotation can align the rotation axis with the vector  $(1, 1, 0)$ . By setting the initial conditions  $\psi(0) = -x_1$  and  $\psi_s(0) = 0$ , we obtain another solution to (1.5) given by

$$(1 - \cos \theta)\psi = -2k_g$$

with the relation

$$\frac{d\theta}{ds} = \frac{1}{\psi}.$$

Due to the presence of divergent improper integrals at singular points, we are unable to derive a specific analytical expression for the variation of the angle

$\theta$ . Nevertheless, numerical calculations (depicted in the left-hand side of Fig. 4) reveal that when the starting point is set at  $\psi = -x_1$  and  $\theta = \pi$ , the angle  $\theta(T, \lambda)$  at the endpoint of the initial first period strictly monotonically increases from  $2\pi$  to  $3\pi$  as  $\lambda$  varies from 0 to  $+\infty$ . This enables us to clearly comprehend the potential behavior of this type of soliton solution on the light-cone.

For  $\mu < 0$ , a suitable rotation can align the rotation axis with the  $z$ -axis, yielding another solution to (1.5) is

$$\psi \sin \theta = \frac{-k_g}{\sqrt{-\mu}}$$

and

$$\frac{d\theta}{ds} = \frac{1}{\psi}.$$

Again, due to the divergent improper integrals at singular points, we are unable to derive an explicit analytical expression for the variation of  $\theta$ . Similarly, numerical calculations (depicted in the right-hand side of Fig. 4) offer further insights: when the starting point is set at  $\psi = -x_1$  and  $\theta = \frac{\pi}{2}$ , the angle  $\theta(T, \lambda)$  at the endpoint of the initial first period strictly monotonically increases from  $2\pi$  to  $\frac{5\pi}{2}$  as  $\lambda$  varies from  $3(\mu/2)^{2/3}$  to  $+\infty$ . This also allows us to clearly understand the potential behavior of this type of soliton solution on the light-cone.

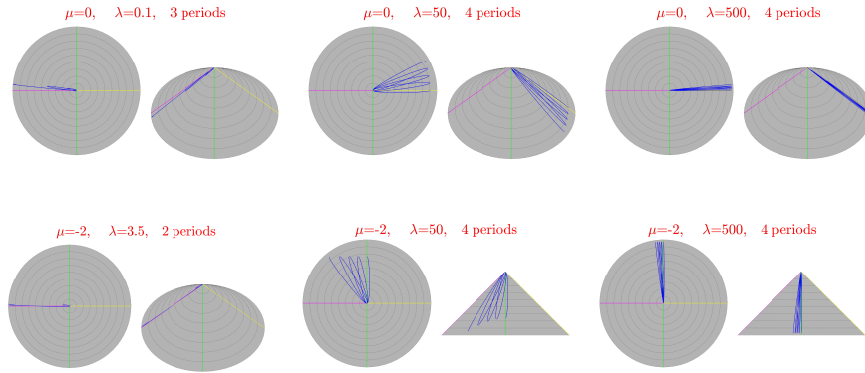


FIGURE 2. The non-closed periodic solitons on light-cone.

Fig. 2 provides a visual representation of solitons rotating around the light-like axis  $(1, 1, 0)$  and the  $z$ -axis for  $\mu = 0$  and  $\mu = -2$ , respectively. As detailed in Corollary 4.15 and Corollary 4.20, the endpoints of each periodic cycle are situated at  $(2n\pi, 3n\pi)$  and  $\left(2n\pi, \frac{(4n+1)\pi}{2}\right)$ , respectively. As  $n$  increases, the endpoints approach  $2n\pi$ . In the first row of Fig. 2, the magenta line represents the rotation axis  $(1, 1, 0)$  with a fixed point situated

at  $\psi = \frac{1}{\lambda}$ . Additionally, the yellow line is positioned at  $\theta = \pi$ . The pattern is very evident: as  $\lambda$  diminishes towards 0, the endpoints of the trajectories draw nearer to the magenta line. Conversely, as  $\lambda$  augments, The endpoint of each cycle moves closer to the yellow line. A comparable trend is clear in the second row of Fig. 2: as  $\lambda$  diminishes towards 3, the endpoints of the trajectories draw nearer to the magenta line. Conversely, as  $\lambda$  increases, the endpoint of each cycle migrates towards the starting point of the trajectories.

With the hints from the previous three special solutions, for (1.5), we can present the general form of the solution (see Section 4.4 for the proof).

**Theorem 1.4.** *Consider three constants  $x_1, x_2$  and  $x_3$  that adhere to the conditions  $x_1 + x_2 + x_3 = 0$  and  $x_1 < x_2 < x_3$ . Define the function*

$$f(s) = x_1 + (x_2 - x_1) \operatorname{sn} \left( \frac{\sqrt{x_3 - x_1}}{2} s, \sqrt{\frac{x_2 - x_1}{x_3 - x_1}} \right)^2.$$

*Then the second order differential equation*

$$\psi_{ss} - \frac{\psi_s^2 + 1}{2\psi} - f(s)\psi = 0,$$

*admits the solution*

$$(-c_1 + c_2 \cos \theta + c_3 \sin \theta)\psi = f(s),$$

*where the integral constants  $c_1, c_2, c_3$  fulfill the relation  $-c_1^2 + c_2^2 + c_3^2 = -x_1 x_2 x_3$ , and  $\theta = \int_0^s \frac{dt}{\psi(t)}$ .*

Specifically, utilizing the curvature formula provided in (2.6), (1.5) can be reconfigured into

$$2\psi_{\theta\theta}\psi - 3\psi_\theta^2 - 2\psi^5(-c_1 + c_2 \cos \theta + c_3 \sin \theta) - \psi^2 = 0.$$

Based on the comprehensive derivation process outlined previously, it becomes evident that the solutions to this equation over the entire interval can be constructed by rotating the points  $(\psi(\theta), \psi(\theta) \cos \theta, \psi(\theta) \sin \theta)$  in the first period around the axis  $(c_1, c_2, c_3)$ . Consequently, by substituting  $\psi = u^{-2}$ , and combining Proposition 4.14 and Proposition 4.19, the following corollary emerges.

**Corollary 1.5.** *For the ordinary differential equation*

$$u_{\theta\theta} + \frac{1}{2u^5}(-c_1 + c_2 \cos \theta + c_3 \sin \theta) + \frac{u}{4} = 0,$$

*where the constants  $c_1, c_2$  and  $c_3$  cannot all be zero simultaneously, the positive solution  $u(\theta)$  demonstrates the subsequent properties.*

- *If  $-c_1^2 + c_2^2 + c_3^2 < 0$ , there exist two positive constant  $D_1$  and  $D_2$  such that  $D_1 \leq u(\theta) \leq D_2$ .*
- *If  $-c_1^2 + c_2^2 + c_3^2 \geq 0$ ,  $u(\theta)$  is unbounded and its infimum is 0.*

*Notably, when  $-c_1^2 + c_2^2 + c_3^2 = 0$ , there exists a fixed point  $u(\theta_0) = u(\theta_0 + 2\pi)$ , where  $\theta_0$  satisfies the conditions  $c_1 \sin \theta_0 = c_2$  and  $c_1 \cos \theta_0 = c_3$ .*



**Outline.** In Section 2, we dedicate some time to revisiting the geometry of the light-cone and introducing our notations. Moving on to Section 3, we derive the relevant evolution equations, ultimately establishing the Li-Yau Harnack inequality for heat flow and highlighting some fascinating properties related to a third-order flow. Then, in Section 4, we deduce the space-periodic solitons for this third-order flow and subsequently obtain analytic solutions to a second-order nonlinear ordinary differential equation.

**Acknowledgements.** This work was supported by Foreign Expert Key Support Program (Northeast Special) Grants-D20240219.

## 2. PRELIMINARIES

Let  $V$  be an  $n$ -dimensional real vector space. A *Lorentzian scalar product* on  $V$  is defined as a non-degenerate symmetric bilinear form  $\langle \cdot, \cdot \rangle_L$  of index 1. This implies the existence of a basis  $\mathbf{e}_1, \dots, \mathbf{e}_n$  of  $V$  such that

$$\langle \mathbf{e}_i, \mathbf{e}_j \rangle_L = \begin{cases} -1, & \text{if } i = j = 1, \\ 1, & \text{if } i = j = 2, \dots, n, \\ 0, & \text{otherwise.} \end{cases}$$

A *Lorentzian manifold* is a pair  $(M, g)$ , where  $M$  is an  $n$ -dimensional smooth manifold and  $g$  is a Lorentzian metric, i.e.,  $g$  associates to each point  $p \in M$  a Lorentzian scalar product  $g_p$  on the tangent space  $T_p M$ .

The *Minkowski space*  $\mathbb{E}_1^n$  is the vector space  $\mathbb{R}^n$  endowed with the Lorentzian scalar product defined as follows:

$$\langle \mathbf{u}, \mathbf{v} \rangle_L = -u_1 v_1 + u_2 v_2 + \dots + u_n v_n, \quad (2.1)$$

where  $\mathbf{u} = (u_1, \dots, u_n) \in \mathbb{R}^n$  and  $\mathbf{v} = (v_1, \dots, v_n) \in \mathbb{R}^n$ . In cartesian coordinates  $(x_1, \dots, x_n)$  on  $\mathbb{R}^n$ , the *Minkowski metric* is defined by  $g = -(dx_1)^2 + (dx_2)^2 + \dots + (dx_n)^2$ .

In Minkowski space  $\mathbb{E}_1^n$ , a vector  $\mathbf{v} = \{v_1, \dots, v_n\} \in \mathbb{E}_1^n$  is classified as follows:

- It is called *space-like* if  $\langle \mathbf{v}, \mathbf{v} \rangle_L > 0$  or if  $\mathbf{v} = \mathbf{0}$ .
- It is termed *time-like* if  $\langle \mathbf{v}, \mathbf{v} \rangle_L < 0$ .
- It is designated as *light-like* (or *null*) if  $\langle \mathbf{v}, \mathbf{v} \rangle_L = 0$  and  $\mathbf{v} \neq \mathbf{0}$ .
- It is considered *causal*, if it is time-like or space-like.

The magnitude (or length) of the vector  $\mathbf{v}$  is denoted by  $|\mathbf{v}|$  and is defined as by  $|\mathbf{v}| = \sqrt{|\langle \mathbf{v}, \mathbf{v} \rangle_L|}$ .

Furthermore, for a curve  $\mathbf{r} = \mathbf{r}(p) : I \subset \mathbb{R} \rightarrow \mathbb{E}_1^n$ , it is classified as space-like, time-like, or light-like, if its velocity vector  $\mathbf{r}'(p)$  is space-like, time-like, or light-like, respectively.

The *plane* with *pseudo-normal*  $\mathbf{v}$  in  $\mathbb{E}_1^n$  is defined by

$$P(\mathbf{v}, c) = \{\mathbf{x} \in \mathbb{E}_1^n \mid \langle \mathbf{x}, \mathbf{v} \rangle_L = c\},$$

where  $\mathbf{v}$  is a non-zero vector in  $\mathbb{E}_1^n$  and  $c$  is constant. Moreover,  $P(\mathbf{v}, c)$  is called a space-like plane, a time-like plane or light-like plane if  $\mathbf{v}$  is time-like, space-like or light-like, respectively.

Given a real number  $c > 0$ , we define the following subspaces in Minkowski space  $\mathbb{E}_1^n$ .

- The *hyperbolic space*  $H^{n-1}(c)$  is given by

$$H^{n-1}(c) = \{\mathbf{x} \in \mathbb{E}_1^{n-1} \mid \langle \mathbf{x}, \mathbf{x} \rangle_L = -c^2\}.$$

- The *de Sitter space*  $S_1^{n-1}(c)$  is defined as

$$S_1^{n-1}(c) = \{\mathbf{x} \in \mathbb{E}_1^n \mid \langle \mathbf{x}, \mathbf{x} \rangle_L = c^2\}.$$

- The *light-cone*  $LC$  is described by

$$LC = \{\mathbf{x} \in \mathbb{E}_1^n \setminus \{0\} \mid \langle \mathbf{x}, \mathbf{x} \rangle_L = 0\}.$$

In  $\mathbb{E}_1^n$ , the term pseudo-sphere collectively refers to the hyperbolic space, the de Sitter space, and the light-cone.

The *arc length parameter* of a curve  $\mathbf{r}(p) \in \mathbb{E}_1^n$  is defined by

$$\frac{ds}{dp} = \left| \frac{d\mathbf{r}}{dp} \right|.$$

Assume  $\mathbf{r}$  be a curve in  $\mathbb{E}_1^n$  parametered with arc length  $s$ , the unit tangent vector  $\mathbf{T}$  is denoted by  $\mathbf{T} = \frac{d\mathbf{r}}{ds} = \mathbf{r}_s$ . In  $\mathbb{E}_1^3$ , the pseudo vector product of  $\mathbf{u}$  and  $\mathbf{v}$  is given by

$$\mathbf{u} \times_L \mathbf{v} = (u_3v_2 - u_2v_3, u_3v_1 - u_1v_3, u_1v_2 - u_2v_1). \quad (2.2)$$

**2.1. The Frenet formulas in Minkowski space.** In  $\mathbb{E}_1^3$ , based on the characteristics of  $\mathbf{T}_s$ , we categorize our discussion into the following two scenarios.

**Case 1.** If  $\langle \mathbf{T}_s, \mathbf{T}_s \rangle_L \neq 0$ , the unit principal normal vector field is defined as  $\mathbf{N} = \frac{\mathbf{T}_s}{|\mathbf{T}_s|}$ , and the unit binormal vector is given by  $\mathbf{B} = \mathbf{T} \times_L \mathbf{N}$ . Here,  $\langle \mathbf{T}, \mathbf{T} \rangle_L = \eta_1$ ,  $\langle \mathbf{N}, \mathbf{N} \rangle_L = \eta_2$ , and  $\langle \mathbf{B}, \mathbf{B} \rangle_L = \eta_3$ , where  $\eta_i = \pm 1$ ,  $i = 1, 2, 3$ . Note that according to (2.1) and (2.2), we have

$$\eta_1\eta_2\eta_3 = -1, \quad \eta_1 + \eta_2 + \eta_3 = 1.$$

The Frenet formula is expressed as (see [Walrave 1995] for more details)

$$\begin{bmatrix} \mathbf{T}_s \\ \mathbf{N}_s \\ \mathbf{B}_s \end{bmatrix} = \begin{bmatrix} 0 & \kappa & 0 \\ \eta_3\kappa & 0 & \tau \\ 0 & \eta_1\tau & 0 \end{bmatrix} \begin{bmatrix} \mathbf{T} \\ \mathbf{N} \\ \mathbf{B} \end{bmatrix}, \quad (2.3)$$

where  $\kappa, \tau$  are referred to as the curvature and torsion of  $\mathbf{r}$ , respectively.

**Case 2.** If  $\langle \mathbf{T}_s, \mathbf{T}_s \rangle_L = 0$ , the principal normal vector field  $\mathbf{N}$  is defined as  $\mathbf{T}_s$ . The binormal vector field  $\mathbf{B}$  is the unique light-like vector field

perpendicular to  $T$  such that  $\langle N, B \rangle_L = 1$ . The Frenet formula in this case is given by (refer to [Walrave 1995] for further information)

$$\begin{bmatrix} \mathbf{T}_s \\ \mathbf{N}_s \\ \mathbf{B}_s \end{bmatrix} = \begin{bmatrix} 0 & 1 & 0 \\ 0 & \bar{\tau} & 0 \\ -1 & 0 & -\bar{\tau} \end{bmatrix} \begin{bmatrix} \mathbf{T} \\ \mathbf{N} \\ \mathbf{B} \end{bmatrix}. \quad (2.4)$$

**2.2. The Frenet formulas on light-cone.** Let us consider the Frenet-Serret type formulae of curve  $\mathbf{r}$  on light-cone  $LC$  in  $\mathbb{E}_1^3$ . In this paper, our primary focus is on curves that lie on the light-cone. It is important to highlight that vectors orthogonal to a light-like vector can only be either light-like or space-like. Furthermore, two light-like vectors are orthogonal to each other if and only if they are linearly dependent. Therefore, throughout the following sections, we will always assume that the unit tangent vector  $\mathbf{T}$  is space-like and  $\frac{ds}{dp} \neq 0$ .

Since  $\mathbf{r}(p)$  is the light-like vector field,  $\frac{d\mathbf{r}}{dp}$  is a space-like vector field perpendicular to  $\mathbf{r}(p)$ . The normal vector field  $\mathbf{Y}$  is the unique light-like vector field perpendicular to  $\mathbf{T}$  such that  $\langle \mathbf{r}, \mathbf{Y} \rangle_L = 1$ . Then the Frenet formula can be expressed by (see [Liu 2004] for more details)

$$\begin{bmatrix} \mathbf{r}_s \\ \mathbf{T}_s \\ \mathbf{Y}_s \end{bmatrix} = \begin{bmatrix} 0 & 1 & 0 \\ k_g & 0 & -1 \\ 0 & -k_g & 0 \end{bmatrix} \begin{bmatrix} \mathbf{r} \\ \mathbf{T} \\ \mathbf{Y} \end{bmatrix}, \quad (2.5)$$

where  $k_g = \langle \mathbf{r}_{ss}, \mathbf{Y} \rangle_L$ .

If  $\langle \mathbf{T}_s, \mathbf{T}_s \rangle_L \neq 0$ , by (2.3) and (2.5), we derive the following relationships

$$k_g = -\eta_2 \frac{k^2}{2}, \quad \tau^2 \kappa^2 = \kappa_s^2.$$

On the other hand, when  $\langle \mathbf{T}_s, \mathbf{T}_s \rangle_L = 0$ , combining of (2.4) and (2.5) gives  $k_g = 0$  and  $\bar{\tau} = 0$ .

In fact, the right half of a light-cone, denoted as  $LC^*$ , can be represented using spherical coordinates as  $(\psi, \psi \cos \theta, \psi \sin \theta)$  with the constraint  $\psi > 0$ , and the curve  $\mathbf{r}$  on light-cone  $LC^*$  can be described by  $\psi = \psi(\theta)$ . A direct computation leads to

$$\begin{aligned} \mathbf{T} &= \frac{1}{\psi} (\psi_\theta, \psi_\theta \cos \theta - \psi \sin \theta, \psi_\theta \sin \theta + \psi \cos \theta), \\ \mathbf{Y} &= \frac{1}{2\psi} \left( -\left(1 + \frac{\psi_\theta^2}{\psi^2}\right), \left(1 - \frac{\psi_\theta^2}{\psi^2}\right) \cos \theta + \frac{2\psi_\theta}{\psi} \sin \theta, \right. \\ &\quad \left. -\frac{2\psi_\theta}{\psi} \cos \theta + \left(1 - \frac{\psi_\theta^2}{\psi^2}\right) \sin \theta \right), \end{aligned}$$

and then

$$\frac{ds}{d\theta} = \psi, \quad k_g = -\frac{\psi^2 + 3\psi_\theta^2 - 2\psi_{\theta\theta}\psi}{2\psi^4}. \quad (2.6)$$

**Proposition 2.1.** *The curve  $\mathbf{r}$  represents the intersection of a plane  $P(\mathbf{v}, 1)$  and  $LC^*$  if and only if the curvature  $k_g$  remains constant, with its value given by  $k_g = \frac{\langle \mathbf{v}, \mathbf{v} \rangle_L}{2}$ . Specifically, if  $\mathbf{r}$  is an ellipse,  $k_g < 0$ ; if  $\mathbf{r}$  is a parabola,  $k_g = 0$ ; and if  $\mathbf{r}$  is a hyperbola,  $k_g > 0$ .*

*Proof.* Assume  $\mathbf{v} = (v_1, v_2, v_3)$ , and then the equation of the plane is  $-v_1\psi + v_2\psi \cos \theta + v_3 \sin \theta = 1$ . Solving for  $\psi$ , we find

$$\psi = \frac{1}{-v_1 + v_2 \cos \theta + v_3 \sin \theta}.$$

Substituting this expression into the formula for the curvature (2.6) and performing the necessary calculations, we obtain  $k_g = \frac{\langle \mathbf{v}, \mathbf{v} \rangle_L}{2}$ .

On the other hand, the nature of  $\mathbf{v}$  determines the type of curve  $\mathbf{r}$ . If  $\mathbf{v}$  is time-like,  $\mathbf{r}$  is an ellipse; if  $\mathbf{v}$  is light-like,  $\mathbf{r}$  is a parabola; and if  $\mathbf{v}$  is space-like,  $\mathbf{r}$  is a hyperbola.

Conversely, if  $k_g$  is constant, we can select three constants  $c_1, c_2$  and  $c_3$  (not all zero) such that  $-c_1^2 + c_2^2 + c_3^2 = 2k_g$ . Then  $\psi = \frac{1}{-c_1 + c_2 \cos \theta + c_3 \sin \theta}$  is the general solution of the curvature equation (2.6). This, in turn, implies that  $\mathbf{r}$  is a planar curves.  $\square$

In  $\mathbb{E}_1^3$ , the rotation matrices around the  $x$ -axis,  $z$ -axis and light-like axis  $(1, 1, 0)$  are respectively given by

$$\begin{aligned} & \begin{pmatrix} 1 & 0 & 0 \\ 0 & \cos \omega & -\sin \omega \\ 0 & \sin \omega & \cos \omega \end{pmatrix}, \\ & \begin{pmatrix} \cosh \omega & \sinh \omega & 0 \\ \sinh \omega & \cosh \omega & 0 \\ 0 & 0 & 1 \end{pmatrix}, \\ & \begin{pmatrix} 1 + \frac{\omega^2}{2} & -\frac{\omega^2}{2} & \omega \\ \frac{\omega^2}{2} & 1 - \frac{\omega^2}{2} & \omega \\ \omega & -\omega & 1 \end{pmatrix}. \end{aligned} \tag{2.7}$$

The corresponding Killing vector fields are

$$-z\partial_y + y\partial_z, \quad y\partial_x + x\partial_y, \quad z\partial_x + z\partial_y + (x - y)\partial_z.$$

**Lemma 2.2.** *On light-cone  $(\psi, \psi \cos \theta, \psi \sin \theta)$ , the vector fields  $\partial_\theta, \psi \cos \theta \partial_\psi - \sin \theta \partial_\theta, \psi \sin \theta \partial_\psi - (1 - \cos \theta) \partial_\theta$  are Killing vector fields.*

*Proof.* A direct computation shows

$$\partial_\psi = \partial_x + \cos \theta \partial_y + \sin \theta \partial_z, \quad \partial_\theta = -\psi \sin \theta \partial_y + \psi \cos \theta \partial_z.$$

On the other hand,

$$\begin{aligned} -z\partial_y + y\partial_z &= -\psi \sin \theta \partial_y + \psi \cos \theta \partial_z, \\ y\partial_x + x\partial_y &= \psi \cos \theta \partial_x + \psi \partial_y, \\ z\partial_x + z\partial_y + (x-y)\partial_z &= \psi \sin \theta (\partial_x + \partial_y) + \psi(1 - \cos \theta) \partial_z. \end{aligned}$$

It is easy to verify

$$\begin{aligned} -z\partial_y + y\partial_z &= \partial_\theta, \\ y\partial_x + x\partial_y &= \psi \cos \theta \partial_\psi - \sin \theta \partial_\theta, \\ z\partial_x + z\partial_y + (x-y)\partial_z &= \psi \sin \theta \partial_\psi - (1 - \cos \theta) \partial_\theta. \end{aligned}$$

□

For the convenience of the subsequent discussion, we introduce the following notations in advance. Let  $\Pi$  represent the elliptic integral of the third kind, defined as

$$\begin{aligned} \Pi(\varphi, \alpha^2, k) &= \int_0^\varphi \frac{d\theta}{(1 - \alpha^2 \sin^2 \theta) \sqrt{1 - k^2 \sin^2 \theta}} \\ &= \int_0^{\sin \varphi} \frac{dt}{(1 - \alpha^2 t^2) \sqrt{(1 - k^2 t^2)(1 - t^2)}}. \end{aligned}$$

Additionally, the elliptic integral of the first kind and the complete elliptic integral of the first kind are respectively expressed as

$$F(\varphi, k) = \Pi(\varphi, 0, k), \quad K(k) = F\left(\frac{\pi}{2}, k\right).$$

### 3. THE EVOLUTIONS OF CURVES ON LIGHT-CONE

Let us next investigate the evolutionary processes of curves on  $LC^*$ . We study a time-dependent family of smooth, local embedded, curves on  $LC^*$ , evolving by the flow:

$$\frac{\partial \mathbf{r}}{\partial t} = U\mathbf{r} + V\mathbf{Y} + W\mathbf{T}.$$

Then  $\langle \mathbf{r}, \mathbf{r} \rangle_L = 0$  and  $\langle \mathbf{r}, \mathbf{Y} \rangle_L = 1$  gives  $V = 0$ , which simplifies the evolution equation to

$$\frac{\partial \mathbf{r}}{\partial t} = U\mathbf{r} + W\mathbf{T}.$$

According to  $g^2 = \langle \mathbf{r}_p, \mathbf{r}_p \rangle_L$  and (2.5), we find

$$\begin{aligned} gg_t &= \langle \mathbf{r}_{pt}, \mathbf{r}_p \rangle_L \\ &= g^2 \langle (U\mathbf{r} + W\mathbf{T})_s, \mathbf{T} \rangle_L \\ &= g^2 (U + W_s). \end{aligned}$$

From this, we obtain

$$\frac{g_t}{g} = U + W_s. \quad (3.1)$$

Furthermore, we have the following derivatives

$$\begin{aligned}\mathbf{T}_t &= (U_s + Wk_g)\mathbf{r} - W\mathbf{Y}, \\ \mathbf{Y}_t &= -(W_s + Wk_g)\mathbf{T} - U\mathbf{Y}.\end{aligned}$$

Concurrently, we compute

$$(k_g)_t = (\langle \mathbf{T}_s, \mathbf{Y} \rangle_L)_t = \langle \mathbf{T}_{st}, \mathbf{Y} \rangle_L + \langle \mathbf{T}_s, \mathbf{Y}_t \rangle_L,$$

which yields

$$(k_g)_t = U_{ss} - 2k_g U + W(k_g)_s. \quad (3.2)$$

Using (3.1) and (3.2), we establish the following lemma

**Lemma 3.1.** *On  $LC^*$ , a vector field  $\mathbf{J} = U\mathbf{r} + W\mathbf{T}$  is designated as a Killing vector field along  $\mathbf{r}$  if and only if it satisfies the following conditions:*

$$\begin{aligned}U + W_s &= 0, \\ U_{ss} - 2k_g U + W(k_g)_s &= 0.\end{aligned}$$

**3.1. Harnack inequality on light-cone.** In particular, for the geometric heat equation on light-cone

$$\frac{\partial \mathbf{r}}{\partial t} = k_g \mathbf{r},$$

we have

$$\frac{g_t}{g} = k_g, \quad (k_g)_t = (k_g)_{ss} - 2k_g^2.$$

Now let  $k = -k_g$ , and we obtain

$$\frac{g_t}{g} = -k, \quad k_t = k_{ss} + 2k^2. \quad (3.3)$$

**Lemma 3.2.** *If  $k$  satisfies (3.3), then  $k_{\min}(t) = \inf_s \{k(s, t)\}$  is a nondecreasing function.*

Let us here give the proof of Theorem 1.2.

*Proof of Theorem 1.2.* Define the Harnack quantity

$$Q := \frac{k_{ss}}{k} - \frac{k_s^2}{k^2} + k.$$

Then

$$k_{ss} = kQ + \frac{k_s^2}{k} - k^2,$$

and by (3.3) we have

$$k_t = kQ + \frac{k_s^2}{k} + k^2.$$

Using the commutation relation  $[\partial_t, \partial_s] = k\partial_s$ , we have

$$\begin{aligned}k_{st} &= k_{ts} + kk_s = Q_s k + 3Qk_s + \frac{k_s^3}{k^2} + kk_s, \\ k_{sst} &= kQ_{ss} + 4Q_s k_s + 3kQ^2 + \left(\frac{6k_s^2}{k} - k^2\right)Q + \frac{k_s^4}{k^3} - 2k^3.\end{aligned}$$

Thus,

$$Q_t = \frac{k_{sst}}{k} - \frac{k_{ss}k_t}{k^2} - \frac{2k_s k_{st}}{k^2} + \frac{2k_s^2 k_t}{k^3} + k_t \triangleq \sum_{j=1}^5 I_j, \quad (3.4)$$

where

$$\begin{aligned} I_1 &= \frac{k_{sst}}{k} = Q_{ss} + \frac{4Q_s k_s}{k} + 3Q^2 + \left(\frac{6k_s^2}{k^2} - k\right)Q + \frac{k_s^4}{k^4} - 2k^2, \\ I_2 &= -Q^2 - \frac{2k_s^2}{k^2}Q - \frac{k_s^4}{k^4} + k^2, \\ I_3 &= -\frac{6k_s^2}{k^2}Q - \frac{2k_s}{k}Q_s - \frac{2k_s^4}{k^4} - \frac{2k_s^2}{k}, \\ I_4 &= \frac{2k_s^2}{k^2}Q + \frac{k_s^4}{k^4} + \frac{2k_s^2}{k} \\ I_5 &= kQ + k^2 + \frac{k_s^2}{k}. \end{aligned}$$

Inserting these expressions into (3.4), we arrive at

$$Q_t = Q_{ss} + \frac{2k_s}{k}Q_s + 2Q^2 + \frac{k_s^2}{k} \geq Q_{ss} + \frac{2k_s}{k}Q_s + 2Q^2.$$

Let  $q(t) = -\frac{1}{2(t-t_0)}$ . Then  $q(t)$  solves the associated ODE

$$\frac{dq}{dt} = 2q^2$$

with condition  $\lim_{t \rightarrow t_0} q(t) = -\infty$  and so the maximum principle gives

$$Q(s, t) \geq q(t), \quad \forall t \in (t_0, T).$$

□

**3.2. A third order curvature flow.** If the curve remains unstretched during its motion, meaning that the distance between any two points on the curve (as measured along the curve itself) remains constant over time, then  $s$  and  $t$  can function as local coordinates on the light-cone. Utilizing equation (3.1), we derive

$$U + W_s = 0,$$

which subsequently allows us to express equation (3.2) as

$$(k_g)_t = U_{ss} - 2k_g U - (k_g)_s \partial^{-1} U.$$

By choosing  $U = (k_g)_s$ , we obtain the KdV equation

$$(k_g)_t = (k_g)_{sss} - 3k_g(k_g)_s.$$

Assume the curvature  $k_g$  is periodic with the parameter  $s$ , that is,  $k_g(s + T, t) = k_g(s, t)$ , where  $T$  is its period. We can verify that

$$\frac{d}{dt} \int_0^T ds = 0, \quad \frac{d}{dt} \int_0^T k_g ds = 0, \quad \frac{d}{dt} \int_0^T k_g^2 ds = 0.$$

#### 4. THE SOLITON SOLUTIONS FOR THE THIRD ORDER CURVATURE FLOW

Now let us consider the solitons for the flow (1.3). Solitons of the geometric flow represent self-similar solutions that maintain their shape under the evolution induced by the flow. To formulate the definition of a soliton, let  $N^n$  be a  $n$ -dimensional Riemannian manifold with metric  $g$ , equipped with a Killing vector field  $\mathbf{J}$  related to an isometry group  $\varphi : N \times \mathbb{R} \rightarrow N$ . The isometry group  $\varphi$  characterizes transformations that preserve the metric  $g$  and hence the geometric properties of the manifold. The relationship between  $\mathbf{J}$  and  $\varphi$  is given by the following differential equation and initial condition

$$\begin{aligned} \frac{d\varphi(x,t)}{dt} &= \mathbf{J}(\varphi(x,t)), \\ \varphi(x,0) &= x. \end{aligned}$$

Here,  $\frac{d\varphi(x,t)}{dt}$  denotes the time derivative of the point  $\varphi(x,t)$  in the direction of the flow induced by the Killing vector field  $\mathbf{J}$ . The initial condition  $\varphi(x,0) = x$  signifies that at time  $t = 0$ , the isometry group leaves each point  $x$  in  $N^n$  unchanged.

A curve  $\mathbf{r}$  on  $LC^*$  is a soliton of the geometric flow (1.1) if, under the action of the isometry group  $\varphi$  parameterized by the flow induced by  $\mathbf{J}$ , the curve evolves in such a way that its shape remains constant up to reparametrization. This property ensures that the soliton maintains its geometric characteristics throughout the evolution process.

Hence, by using  $U = (k_g)_s$  and  $W = -k_g$ , we have

$$(k_g)_{sss} - 3k_g(k_g)_s = 0.$$

Through integration, we obtain

$$(k_g)_{ss} - \frac{3}{2}k_g^2 + \frac{\lambda}{2} = 0, \quad ((k_g)_s)^2 - k_g^3 + \lambda k_g + \mu = 0,$$

where  $\lambda$  and  $\mu$  are the integration constants.

**Remark 4.1.** The trivial solution to (1.4) occurs when  $k_g$  is constant. Through direct computation, it is evident that (1.4) possesses nontrivial periodic solutions if and only if the cubic equation  $x^3 - \lambda x - \mu = 0$  has three distinct real roots. This condition is satisfied when  $\lambda > 3\left(\frac{\mu}{2}\right)^{2/3}$ .

Thus, the three solutions of cubic equation  $x^3 - \lambda x - \mu = 0$  are

$$\begin{aligned} x_1 &= -\frac{2\sqrt{3\lambda}}{3} \cos \frac{\theta}{3}, \\ x_2 &= \frac{2\sqrt{3\lambda}}{3} \cos \frac{\theta + \pi}{3}, \\ x_3 &= \frac{2\sqrt{3\lambda}}{3} \cos \frac{\theta - \pi}{3}, \end{aligned}$$



where  $\theta = \arccos \left( -\frac{\mu}{2} \cdot \left( \frac{3}{\lambda} \right)^{3/2} \right)$  and  $x_1 < x_2 < x_3$ .

**Remark 4.2.** If  $\lambda > 3 \left( \frac{\mu}{2} \right)^{2/3}$ , the periodic solutions for (1.4) can be expressed in terms of the Jacobi elliptic sine function

$$k_g = x_1 + (x_2 - x_1) \operatorname{sn}^2 \left( \frac{\sqrt{x_3 - x_1}}{2} s, \sqrt{\frac{x_2 - x_1}{x_3 - x_1}} \right).$$

**Remark 4.3.** By invoking (2.6), the task of identifying periodic solitons for the flow described by (1.3) is now equivalent to solving the equation

$$\psi_{ss} - \frac{\psi_s^2 + 1}{2\psi} - \left( x_1 + (x_2 - x_1) \operatorname{sn}^2 \left( \frac{\sqrt{x_3 - x_1}}{2} s, \sqrt{\frac{x_2 - x_1}{x_3 - x_1}} \right) \right) \psi = 0.$$

In what follows, we employ the Killing vector field to derive analytic solutions for this second-order nonlinear differential equation.

**4.1. Solitons rotating around a time-like axis.** In fact, a periodic curve can be generated by rotating the initial curve through one full period around an axis. The crucial step lies in determining the appropriate rotation matrix. If the rotation axis is time-like, we can always assume, through a suitable rotation, that this axis aligns with the  $x$ -axis. Consequently, the rotation matrix can be expressed as

$$\begin{pmatrix} 1 & 0 & 0 \\ 0 & \cos \omega & -\sin \omega \\ 0 & \sin \omega & \cos \omega \end{pmatrix}.$$

**Proposition 4.4.** *If the solitons rotate around the  $x$ -axis, then  $\mu > 0$  and  $\psi$  is given by  $\psi = -\frac{k_g}{\sqrt{\mu}}$ .*

*Proof.* By Lemma 3.1 and (1.4), we discover

$$\mathbf{J} = (k_g)_s \mathbf{r} - k_g \mathbf{T}$$

constitutes a Killing vector field along the curve  $\mathbf{x}$ . Now we can employ the coordinates  $\mathbf{r}(\theta, \psi) = (\psi, \psi \cos \theta, \psi \sin \theta)$ , so that according to Lemma 2.2 its equator gives the only integral curve around  $x$ -axis of  $\mathbf{J} : \partial_\theta = b\mathbf{J}$ . Taking the inner product of both sides of this equation with  $\mathbf{T}$  generates

$$\psi = -bk_g.$$

Let  $\bar{\mathbf{r}}$  denote the integral curve of vector field  $\bar{\mathbf{T}} = \frac{\mathbf{J}}{|\mathbf{J}|}$ . Specifically,

$$\bar{\mathbf{T}} = \frac{(k_g)_s}{k_g} \mathbf{r} - \mathbf{T}.$$

Therefore at the point where  $(k_g)_s = 0$ , we need to find the derivative

$$\bar{\mathbf{T}}_{\bar{s}} = \frac{ds}{d\bar{s}} \left( \frac{(k_g)_{ss}k_g - k_g^3}{k_g^2} \mathbf{r} + \mathbf{N} \right).$$

At that given point, we have  $\mathbf{r} = \bar{\mathbf{r}}$ , which implies

$$\frac{ds}{d\bar{s}} = -1.$$

Accordingly, by (1.4) and  $(k_g)_s = 0$ ,

$$\bar{k}_g = -\frac{(k_g)_{ss}k_g - k_g^3}{k_g^2} = -\frac{k_g^3 - \lambda k_g}{2k_g^2} = -\frac{\mu}{2k_g^2}.$$

On the other hand, based on Proposition 2.1, the curvature of the plane curve that is perpendicular to the  $x$ -axis is given by  $\bar{k}_g = -\frac{1}{2\psi^2}$ . Consequently, we can derive

$$\mu > 0, \quad \text{and} \quad \frac{1}{b} = \sqrt{\mu}.$$

□

The following theorem provides the detailed expression for  $\omega$ .

**Theorem 4.5.** *If  $\mu > 0$ , by a rotation, then the progression angle  $\Lambda^\Theta$  in one period of the curvature can be expressed as follows*

$$\Lambda^\Theta = -2\sqrt{\mu} \int_{x_1}^{x_2} \frac{1}{x\sqrt{x^3 - \lambda x - \mu}} dx. \quad (4.1)$$

*Proof.* It is straightforward to observe that in one period, the arc length  $T$  is given by

$$T = 2 \int_{x_1}^{x_2} \frac{1}{\sqrt{x^3 - \lambda x - \mu}} dx = \frac{4}{\sqrt{x_3 - x_1}} K \left( \sqrt{\frac{x_2 - x_1}{x_3 - x_1}} \right),$$

where  $K$  denotes the complete elliptic integral of the first kind. By Proposition 4.4,  $\frac{d\theta}{ds} = \frac{1}{\psi}$  in (2.6), and (1.4), we have

$$\Lambda^\Theta = -\sqrt{\mu} \int_0^T \frac{1}{k_g} ds = -2\sqrt{\mu} \int_{x_1}^{x_2} \frac{1}{x\sqrt{x^3 - \lambda x - \mu}} dx, \quad (4.2)$$

which achieves the anticipated outcome. □

**Remark 4.6.** If  $\mu > 0$ , by selecting the initial conditions  $\psi(0) = \frac{-x_1}{\sqrt{\mu}}$  and  $\psi_s(0) = 0$ , we obtain the solution to equation (1.5) as follows

$$\psi = \frac{x_1 + (x_2 - x_1) \operatorname{sn}^2 \left( \frac{\sqrt{x_3 - x_1}}{2} s, \sqrt{\frac{x_2 - x_1}{x_3 - x_1}} \right)}{\sqrt{\mu}}.$$

**Remark 4.7.** If  $\mu \leq 0$ , then Proposition 4.4 implies that the curve cannot be rotated around the time-like axis. According to the rotation matrix (2.7), the curves rotation round the space-like or light-like axis can not result in the formation of closed curves. It is only when  $\mu > 0$  that the solitons are capable of forming closed curves.

Based on [Gradshteyn and Ryzhik 2014], we obtain an elegant expression for (4.1), that is,

$$\Lambda^\Theta = \frac{4\sqrt{\mu}}{-x_1\sqrt{x_3-x_1}} \Pi\left(\frac{\pi}{2}, \frac{x_2-x_1}{-x_1}, \sqrt{\frac{x_2-x_1}{x_3-x_1}}\right).$$

**Proposition 4.8.** Assume  $\mu > 0$ . Then,

- (1) as  $\lambda \rightarrow 3\left(\frac{\mu}{2}\right)^{2/3}$ ,  $\Lambda^\Theta \rightarrow 2\sqrt{2/3}\pi$ ;
- (2) as  $\lambda \rightarrow +\infty$ ,  $\Lambda^\Theta \rightarrow 2\pi$ .

*Proof.* For  $\lambda \rightarrow 3\left(\frac{\mu}{2}\right)^{2/3}$ , we have

$$x_1 \rightarrow -\frac{\sqrt{3\lambda}}{3}, \quad x_2 \rightarrow -\frac{\sqrt{3\lambda}}{3}, \quad x_3 \rightarrow \frac{2\sqrt{3\lambda}}{3}.$$

Through  $\Pi\left(\frac{\pi}{2}, 0, 0\right) = \frac{\pi}{2}$ , we get  $\Lambda^\Theta \rightarrow 2\sqrt{2/3}\pi$ .

For  $\lambda \rightarrow +\infty$ , we have

$$\theta \rightarrow \frac{\pi}{2}, \quad x_1 \rightarrow -\infty, \quad x_3 \rightarrow +\infty.$$

Since  $x_1x_2x_3 = \mu$  and  $x_1 + x_2 + x_3 = 0$ , it is easy to find

$$x_2 \rightarrow 0, \quad \frac{x_1}{x_3} = -1, \quad x_1^2x_2 \rightarrow -\mu, \quad \alpha^2 \rightarrow 1, \quad k^2 \rightarrow \frac{1}{2},$$

where  $\alpha^2 = \frac{x_2-x_1}{-x_1}$ ,  $k^2 = \frac{x_2-x_1}{x_3-x_1}$ . According to [Byard and Friedman 1971], we obtain the expansion

$$\begin{aligned} \int_0^{\frac{\pi}{2}} \frac{d\theta}{(1-\alpha^2\sin^2\theta)\sqrt{1-k^2\sin^2\theta}} &= \int_0^{\frac{\pi}{2}} \frac{d\theta}{\sqrt{1-k^2\sin^2\theta}} \\ &+ \frac{1}{1-k^2} \int_0^{\frac{\pi}{2}} \sqrt{1-k^2\sin^2\theta} d\theta \\ &+ \frac{(2-k^2(1+\alpha^2))\pi}{4(1-k^2)\sqrt{1-k^2}\sqrt{1-\alpha^2}} \\ &+ O(1-\alpha^2), \end{aligned}$$

where  $\alpha^2 \neq 1$  and  $O(1-\alpha^2)$  signifies that the remaining terms are bounded by  $(1-\alpha^2)C$  for some constant  $C$ . One can verify that

$$\lim_{k^2 \rightarrow \frac{1}{2}} \int_0^{\frac{\pi}{2}} \frac{d\theta}{\sqrt{1-k^2\sin^2\theta}} = 0, \quad \lim_{k^2 \rightarrow \frac{1}{2}} \int_0^{\frac{\pi}{2}} \sqrt{1-k^2\sin^2\theta} d\theta = 0.$$

Direct computation shows

$$\lim_{\lambda \rightarrow +\infty} \frac{(2 - k^2(1 + \alpha^2))\pi}{4(1 - k^2)\sqrt{1 - k^2}\sqrt{1 - \alpha^2}} \times \frac{4\sqrt{\mu}}{-x_1\sqrt{x_3 - x_1}} = 2\pi.$$

Hence, we complete the proof.  $\square$

Now let us consider the monotonicity of  $\Lambda^\Theta$ .

**Remark 4.9.** If  $\mu > 0$ , we can make  $\mu = 2$  in (1.4). In fact, one can check that this amounts to replacing  $k_g$ ,  $s$  by  $\left(\frac{\mu}{2}\right)^{1/3} \bar{k}_g$ ,  $\left(\frac{\mu}{2}\right)^{-2/3} p$ , respectively. In the following, we only consider the case  $\mu = 2$ .

By series expansions in [Byard and Friedman 1971], if  $k^2 < 1$  and  $k^2 < \alpha^2$ , it follows

$$\Pi(v, k) = \Pi\left(\frac{\pi}{2}, \alpha^2, k\right) = \sum_{m=0}^{\infty} c_m k^{2m}, \quad (4.3)$$

where

$$\begin{aligned} c_0 &= \frac{\pi}{2\sqrt{1 - \alpha^2}}, \\ c_1 &= \frac{\pi}{4\alpha^2} \left( \frac{1}{\sqrt{1 - \alpha^2}} - 1 \right), \\ c_2 &= \frac{3\pi}{32\alpha^4} \left( \frac{2}{\sqrt{1 - \alpha^2}} - 2 - \alpha^2 \right), \\ c_3 &= \frac{5\pi}{256\alpha^6} \left( \frac{8}{\sqrt{1 - \alpha^2}} - 8 - 4\alpha^2 - 3\alpha^4 \right), \end{aligned}$$

$$2(m+1)\alpha^2 c_{m+1} = \frac{\pi}{2(2m-1)} \binom{-\frac{1}{2}}{m}^2 + (1-2m)c_{m-1} + (2m+1+2mv)c_m,$$

and  $\binom{-\frac{1}{2}}{m}$  is the binomial coefficient. Let  $x = (3/\lambda)^{3/2}$ , and then

$$\begin{aligned} \frac{4\sqrt{\mu}}{-x_1\sqrt{x_3 - x_1}} c_0 &= \sqrt{2}\pi + \frac{\sqrt{6}}{18}\pi x + O(x^2), \\ \frac{4\sqrt{\mu}}{-x_1\sqrt{x_3 - x_1}} c_1 k^2 &= \frac{\sqrt{2}}{4}\pi - \frac{\sqrt[4]{3}}{6}\pi x^{1/2} - \frac{\sqrt{6}}{72}\pi x + O(x^2), \\ \frac{4\sqrt{\mu}}{-x_1\sqrt{x_3 - x_1}} c_2 k^4 &= \frac{3\sqrt{2}}{32}\pi - \frac{3\sqrt[4]{3}}{32}\pi x^{1/2} - \frac{\sqrt{6}}{64}\pi x + \frac{5\sqrt[4]{27}}{288}\pi x^{3/2} + O(x^2), \\ \frac{4\sqrt{\mu}}{-x_1\sqrt{x_3 - x_1}} c_3 k^6 &= \frac{5\sqrt{2}}{128}\pi - \frac{25\sqrt[4]{3}}{512}\pi x^{1/2} - \frac{25\sqrt{6}}{2304}\pi x \\ &\quad + \frac{125\sqrt[4]{27}}{6912}\pi x^{3/2} + O(x^2), \end{aligned}$$

$$\begin{aligned}
 \frac{4\sqrt{\mu}}{-x_1\sqrt{x_3-x_1}}c_4k^8 &= \frac{35\sqrt{2}}{2048}\pi - \frac{1225\sqrt[4]{3}}{49152}\pi x^{1/2} - \frac{245\sqrt{6}}{36864}\pi x \\
 &\quad + \frac{6125\sqrt[4]{27}}{442368}\pi x^{3/2} + O(x^2), \\
 \frac{4\sqrt{\mu}}{-x_1\sqrt{x_3-x_1}}c_5k^{10} &= \frac{63\sqrt{2}}{8192}\pi - \frac{6615\sqrt[4]{3}}{524288}\pi x^{1/2} - \frac{63\sqrt{6}}{16384}\pi x \\
 &\quad + \frac{1225\sqrt[4]{27}}{131072}\pi x^{3/2} + O(x^2), \\
 \frac{4\sqrt{\mu}}{-x_1\sqrt{x_3-x_1}}c_6k^{12} &= \frac{231\sqrt{2}}{65536}\pi - \frac{53361\sqrt[4]{3}}{8388608}\pi x^{1/2} - \frac{847\sqrt{6}}{393216}\pi x \\
 &\quad + \frac{148225\sqrt[4]{27}}{25165824}\pi x^{3/2} + O(x^2), \\
 \frac{4\sqrt{\mu}}{-x_1\sqrt{x_3-x_1}}c_7k^{14} &= \frac{32947\sqrt{2}}{201326592}\pi - \frac{429429\sqrt[4]{3}}{134217728}\pi x^{1/2} - \frac{1859\sqrt{6}}{1572864}\pi x \\
 &\quad + \frac{715715\sqrt[4]{27}}{201326592}\pi x^{3/2} + O(x^2).
 \end{aligned}$$

Finally,  $\Lambda^\Theta$  can be expressed as

$$\begin{aligned}
 \Lambda^\Theta &= \frac{370345\sqrt{2}}{262144}\pi - \frac{47827845\sqrt[4]{3}}{134217728}\pi x^{1/2} - \frac{715\sqrt{6}}{524288}\pi x \\
 &\quad + \frac{123361315\sqrt[4]{27}}{1811939328}\pi x^{3/2} + O(x^2).
 \end{aligned} \tag{4.4}$$

By the first four parts of this equation, we can see that  $\Lambda^\Theta(\lambda)$  is monotonically increasing when  $\lambda > 3\left(\frac{\mu}{2}\right)^{2/3}$ . By Proposition 4.8, we have  $\Lambda^\Theta(\lambda)$  converges to  $2\pi$  as  $\lambda \rightarrow +\infty$ , and converges to  $2\sqrt{2/3}\pi$  as  $\lambda \rightarrow 3\left(\frac{\mu}{2}\right)^{2/3}$ , which clearly shows  $2\sqrt{2/3}\pi < \Lambda^\Theta(\lambda) < 2\pi$ .

**Remark 4.10.** In Fig. 3, the curves depicting  $\Lambda^\Theta(\lambda)$  are precisely rendered using two distinct methods: the numerical integral approach defined in (4.1), and the approximate series expansions (4.4) with respect to  $\lambda$ . Notably, these two representations exhibit remarkable congruence, with minimal deviations among them, essentially indicating a near-perfect overlap.

**4.2. Solitons rotating around a light-like axis.** If the rotation axis is light-like, it is always possible, through an appropriate rotation, to assume it aligns with the vector  $(1, 1, 0)$ . Consequently, the corresponding rotation matrix can be formulated as

$$\begin{pmatrix} 1 + \frac{\omega^2}{2} & -\frac{\omega^2}{2} & \omega \\ \frac{\omega^2}{2} & 1 - \frac{\omega^2}{2} & \omega \\ \omega & -\omega & 1 \end{pmatrix}. \tag{4.5}$$

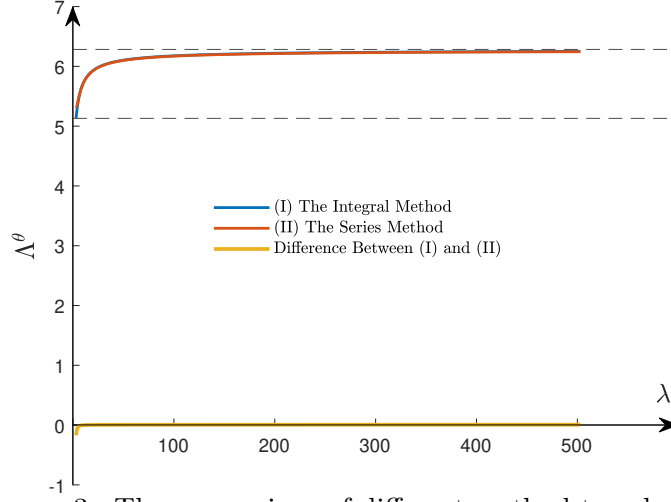


FIGURE 3. The comparison of different method to calculate  $\Lambda^\Theta$ .

**Proposition 4.11.** *When solitons rotate around the light-like axis  $(1, 1, 0)$ , it follows that  $\mu = 0$  and  $\psi$  is given by*

$$(1 - \cos \theta)\psi = -bk_g,$$

where  $b$  denotes an arbitrary positive constant.

*Proof.* By Lemma 3.1 and (1.4), we discover

$$\mathbf{J} = (k_g)_s \mathbf{r} - k_g \mathbf{T}$$

constitutes a Killing vector field along the curve  $\mathbf{x}$ . Now we can employ the coordinates  $\mathbf{x}(\theta, \psi) = (\psi, \psi \cos \theta, \psi \sin \theta)$ , so that according to Lemma 2.2 its equator gives the only integral curve around light-like axis  $(1, 1, 0)$  of  $\mathbf{J} : \psi \sin \theta \partial_\psi - (1 - \cos \theta) \partial_\theta = -b\mathbf{J}$ . Taking the inner product of both sides of this equation with  $\mathbf{T}$  generates

$$(1 - \cos \theta)\psi = -bk_g.$$

Let  $\bar{\mathbf{r}}$  denote the integral curve of vector field  $\bar{\mathbf{T}} = \frac{\mathbf{J}}{|\mathbf{J}|}$ . Similar calculations as in Proposition 4.4, we have

$$\bar{k}_g = -\frac{(k_g)_{ss}k_g - k_g^3}{k_g^2} = -\frac{k_g^3 - \lambda k_g}{2k_g^2} = -\frac{\mu}{2k_g^2}.$$

On the other hand, based on Proposition 2.1, the curvature of the plane curve that is perpendicular to the axis  $(1, 1, 0)$  is given by  $\bar{k}_g = 0$ . Consequently, we can derive  $\mu = 0$ .  $\square$

Then we have

$$\begin{aligned}\sin \theta + (1 - \cos \theta) \psi_s &= -b(k_g)_s, \\ \frac{\cos \theta}{\psi} + \frac{\psi_s}{\psi} \sin \theta + (1 - \cos \theta) \psi_{ss} &= -b(k_g)_{ss}.\end{aligned}$$

**Remark 4.12.** In the first period, the maximum value of  $k_g$  is zero, which we assume is achieved at the point where  $\theta = 2\pi$ . Subsequently, all instances where  $k_g = 0$  arise at  $\theta = 2n\pi$ , where  $n$  is any positive integer. Notably, at these points,  $\psi$  takes on a constant value of  $\frac{2}{b\lambda}$ . Consequently, these points manifest as a same point on the light-cone.

It is straightforward to observe that in one period, the arc length  $T$  is given by

$$T = 2 \int_{-\sqrt{\lambda}}^0 \frac{1}{\sqrt{x^3 - \lambda x}} dx = \frac{4}{\sqrt{2\sqrt{\lambda}}} K \left( \sqrt{\frac{1}{2}} \right),$$

where  $K$  denotes the complete elliptic integral of the first kind.

Now, let us consider the initial conditions  $\psi(0) = -x_1$  and  $\psi_s(0) = 0$ . These conditions imply that  $\theta = \pi$  at  $s = 0$  and  $b = 2$ . Furthermore,

$$\psi \sin^2 \left( \frac{1}{2} \int_0^s \frac{dt}{\psi(t)} + \frac{\pi}{2} \right) = -k_g.$$

Then we have

$$\psi = - \left( 1 + \frac{1}{4} \left( \int_0^s \frac{dt}{k_g(t)} \right)^2 \right) k_g(s).$$

Based on [Gradshteyn and Ryzhik 2014], according to (1.4), we have when  $s < \frac{T}{2}$ ,

$$\begin{aligned}\psi &= - \left( 1 + \frac{1}{4} \left( \int_{x_1}^{k_g(s)} \frac{dx}{x\sqrt{x^3 - \lambda x}} \right)^2 \right) k_g(s) \\ &= - \left( 1 + \frac{1}{2\lambda\sqrt{\lambda}} \left( \Pi \left( \arcsin \sqrt{\frac{k_g(s) + \sqrt{\lambda}}{\sqrt{\lambda}}}, 1, \sqrt{\frac{1}{2}} \right) \right)^2 \right) k_g(s) \\ &= - \left( 1 + \frac{1}{2\lambda\sqrt{\lambda}} \left( \Pi \left( \arcsin \left| \operatorname{sn} \left( \frac{\sqrt[4]{\lambda}}{\sqrt{2}} s, \sqrt{\frac{1}{2}} \right) \right|, 1, \sqrt{\frac{1}{2}} \right) \right)^2 \right) \times \\ &\quad \sqrt{\lambda} \left( -1 + \operatorname{sn}^2 \left( \frac{\sqrt[4]{\lambda}}{\sqrt{2}} s, \sqrt{\frac{1}{2}} \right) \right).\end{aligned}$$

**Remark 4.13.** When  $\mu = 0$ , by specifying the initial conditions  $\psi(0) = -x_1$  and  $\psi_s(0) = 0$ , we find that the solution to equation (1.5) is given by

$$\psi \sin^2 \left( \frac{1}{2} \int_0^s \frac{dt}{\psi(t)} + \frac{\pi}{2} \right) = x_1 \left( -1 + \operatorname{sn}^2 \left( \frac{\sqrt{-x_1}}{\sqrt{2}} s, \sqrt{\frac{1}{2}} \right) \right).$$

Alternatively, if  $s < \frac{T}{2}$ , this can be expressed as

$$\begin{aligned} \psi = & - \left( 1 - \frac{1}{2x_1^3} \left( \Pi \left( \phi, 1, \sqrt{\frac{1}{2}} \right) \right)^2 \right) \times \\ & x_1 \left( 1 - \operatorname{sn}^2 \left( \frac{\sqrt{-x_1}}{\sqrt{2}} s, \sqrt{\frac{1}{2}} \right) \right), \end{aligned}$$

where  $\phi = \operatorname{am} \left( \frac{\sqrt{-x_1}}{\sqrt{2}} s, \sqrt{\frac{1}{2}} \right)$ , and  $\operatorname{am}$  denotes the jacobi amplitude function.

**Proposition 4.14.** *If the solitons rotate around the light-like axis  $(1, 1, 0)$ , then  $\psi$  is unbounded and its infimum is 0.*

*Proof.* By applying the rotation matrix given in (4.5), after  $n$  cycles, points  $(\psi, \psi \cos \theta, \psi \sin \theta)$  in the first cycle are rotated to the points

$$\begin{aligned} & \left( 1 + \frac{(n\omega)^2}{2} - \frac{(n\omega)^2}{2} \cos \theta + n\omega \sin \theta, \right. \\ & \quad \left. \frac{(n\omega)^2}{2} + \left( 1 - \frac{(n\omega)^2}{2} \right) \cos \theta + n\omega \sin \theta, n\omega - n\omega \cos \theta + \sin \theta \right) \psi. \end{aligned}$$

For  $\theta_0 = \pi$ ,  $\psi_n = (1 + (n\omega)^2) \psi_0$ , where  $\psi_0$  is the value for  $\psi$  at  $\theta_0$  in the first period.  $\psi_n$  tends to  $+\infty$  as  $n \rightarrow +\infty$ , which demonstrates that  $\psi$  is unbounded.

Next, we consider the function

$$f(\theta) = 1 + \frac{(n\omega)^2}{2} - \frac{(n\omega)^2}{2} \cos \theta + n\omega \sin \theta.$$

Its derivative is given by

$$f'(\theta) = \frac{(n\omega)^2}{2} \sin \theta + n\omega \cos \theta.$$

Setting  $f'(\bar{\theta}_n) = 0$  leads to

$$\sin \bar{\theta}_n = -\frac{2}{\sqrt{4 + (n\omega)^2}}, \quad \cos \bar{\theta}_n = \frac{n\omega}{\sqrt{4 + (n\omega)^2}}.$$



Furthermore, the second derivative of  $f$  at  $\bar{\theta}_n$  is

$$f''(\bar{\theta}_n) = \frac{(n\omega)^2}{2} \cos \bar{\theta}_n - n\omega \sin \bar{\theta}_n = \frac{n\omega \sqrt{4 + (n\omega)^2}}{2} > 0,$$

indicating that  $\bar{\theta}_n$  is a minimum point of  $f$ . At this minimum point, the value of  $f$  is:

$$f(\bar{\theta}_n) = 1 - \frac{2}{1 + \sqrt{1 + 4/(n\omega)^2}}.$$

As  $n \rightarrow +\infty$ ,  $f(\bar{\theta}_n)$  tends to 0. Therefore, the infimum of  $\psi$  (considering its dependence on  $f(\theta)$  through the rotation) is 0.  $\square$

If  $\theta(0) = \pi$ , according to the preceding proof, we derive the following expressions

$$\sin \theta(nT) = \frac{2n\omega}{1 + (n\omega)^2}, \quad \cos \theta(nT) = \frac{(n\omega)^2 - 1}{1 + (n\omega)^2}.$$

From these expressions, we deduce the following corollary.

**Corollary 4.15.** *When solitons rotate around the light-like axis  $(1, 1, 0)$  with the initial condition  $\theta(0) = \pi$ , it holds that  $2n\pi < \theta(nT) < (2n + 1)\pi$ . The angle  $\theta(nT) - 2n\pi$  decreases monotonically as  $n$  increases, and as the integer  $n$  approaches positive infinity,  $\theta(nT) - 2n\pi$  converges to zero.*

**Remark 4.16.** Given the initial conditions  $\psi(0) = -x_1$  and  $\psi_s(0) = 0$ , our numerical calculations (depicted in the left-hand side of Fig. 4) reveal that  $\theta(T, \lambda)$  exhibits monotonic increasing behavior with respect to  $\lambda$ . Furthermore, we observe that  $\lim_{\lambda \rightarrow 0} \theta(T, \lambda) = 2\pi$ , whereas  $\lim_{\lambda \rightarrow +\infty} \theta(T, \lambda) = 3\pi$ .

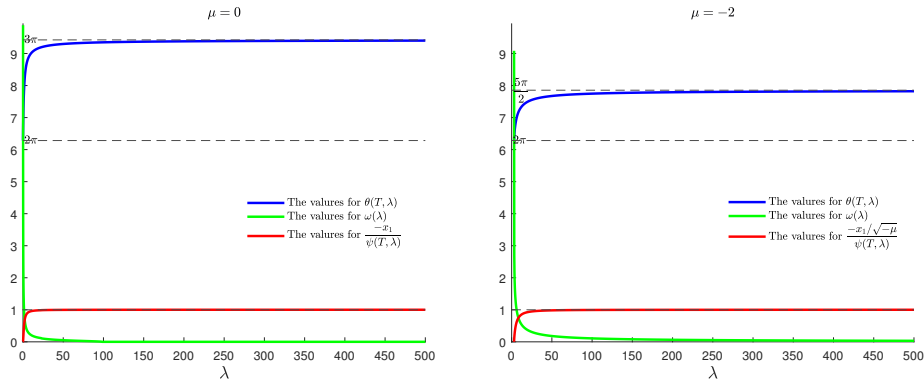


FIGURE 4. Monotonicity & asymptotics at  $s = T$  with varying  $\lambda$ .

**4.3. Solitons rotating around a space-like axis.** If the rotation axis is space-like, we can always assume, through a suitable rotation, that this axis aligns with the  $z$ -axis. Consequently, the rotation matrix can be expressed as

$$\begin{pmatrix} \cosh \omega & \sinh \omega & 0 \\ \sinh \omega & \cosh \omega & 0 \\ 0 & 0 & 1 \end{pmatrix}. \quad (4.6)$$

By employing methodologies akin to those utilized in Proposition 4.4 and Proposition 4.11, we can formulate the subsequent proposition.

**Proposition 4.17.** *If the solitons rotate around the  $z$ -axis, it necessitates that  $\mu < 0$  and  $\psi$  is expressed as*

$$\psi \sin \theta = \frac{-k_g}{\sqrt{-\mu}}.$$

It is straightforward to observe that in one period, the arc length  $T$  is given by

$$T = 2 \int_{x_1}^{x_2} \frac{1}{\sqrt{x^3 - \lambda x - \mu}} dx = \frac{4}{\sqrt{x_3 - x_1}} K \left( \sqrt{\frac{x_2 - x_1}{x_3 - x_1}} \right),$$

where  $K$  denotes the complete elliptic integral of the first kind.

In one period,  $k_g$  demonstrates the presence of two zero points, occurring at  $\theta = \pi$  and  $\theta = 2\pi$ , respectively, due to the condition that  $\psi > 0$ . According to (1.4), we have

$$\cos \theta + \psi_s \sin \theta = \frac{-(k_g)_s}{\sqrt{-\mu}}. \quad (4.7)$$

(1.4) yields  $(k_g)_s = \pm \sqrt{-\mu}$  at  $\theta = \pi$  and  $\theta = 2\pi$ .

Then, we choose the initial condition  $\psi(0) = \frac{-x_1}{\sqrt{-\mu}}$ , which yields  $\theta = \frac{\pi}{2}$  at  $s = 0$ . From (4.7), we deduce that  $\psi_s(0) = 0$ . Given these conditions, we obtain

$$\psi \sin \left( \int_0^s \frac{dt}{\psi(t)} + \frac{\pi}{2} \right) = \frac{-k_g}{\sqrt{-\mu}}.$$

Since  $\theta = \pi$  and  $\theta = 2\pi$  arise in the initial period, the range for  $\theta$  is  $\pi/2 \leq \theta < 3\pi$ , and at the endpoint,  $\theta > 2\pi$ . Once again, utilizing  $\frac{ds}{d\theta} = \psi$

in (2.6), we find when  $s < \frac{2}{\sqrt{x_3 - x_1}} F \left( \arcsin \sqrt{\frac{-x_1}{x_2 - x_1}}, \sqrt{\frac{x_2 - x_1}{x_3 - x_1}} \right)$ ,

$$\psi = \cosh \left( \int_0^s \frac{\sqrt{-\mu}}{k_g(t)} dt \right) \frac{-k_g(s)}{\sqrt{-\mu}}.$$

Based on [Gradshteyn and Ryzhik 2014], according to (1.4), we have

$$\begin{aligned}\psi &= \cosh \left( \sqrt{-\mu} \int_{x_1}^{k_g(s)} \frac{1}{x \sqrt{x^3 - \lambda x - \mu}} dx \right) \frac{-k_g(s)}{\sqrt{-\mu}} \\ &= \cosh \left( \frac{2\sqrt{-\mu}}{x_1 \sqrt{x_3 - x_1}} \Pi \left( \arcsin \sqrt{\frac{k_g - x_1}{x_2 - x_1}}, \frac{x_2 - x_1}{-x_1}, \sqrt{\frac{x_2 - x_1}{x_3 - x_1}} \right) \right) \frac{-k_g(s)}{\sqrt{-\mu}},\end{aligned}$$

$$\text{when } s < \frac{2}{\sqrt{x_3 - x_1}} F \left( \arcsin \sqrt{\frac{-x_1}{x_2 - x_1}}, \sqrt{\frac{x_2 - x_1}{x_3 - x_1}} \right).$$

**Remark 4.18.** When  $\mu < 0$ , by specifying the initial conditions  $\psi(0) = \frac{-x_1}{\sqrt{-\mu}}$  and  $\psi_s(0) = 0$ , we find that the solution to equation (1.5) is given by

$$\psi \sin \left( \int_0^s \frac{dt}{\psi(t)} + \frac{\pi}{2} \right) = - \frac{x_1 + (x_2 - x_1) \text{sn}^2 \left( \frac{\sqrt{x_3 - x_1}}{2} s, \sqrt{\frac{x_2 - x_1}{x_3 - x_1}} \right)}{\sqrt{-\mu}}.$$

Alternatively, when  $s < \frac{2}{\sqrt{x_3 - x_1}} F \left( \arcsin \sqrt{\frac{-x_1}{x_2 - x_1}}, \sqrt{\frac{x_2 - x_1}{x_3 - x_1}} \right)$ , this can be expressed as

$$\begin{aligned}\psi &= - \frac{1}{\sqrt{-\mu}} \cosh \left( \frac{2\sqrt{-\mu}}{x_1 \sqrt{x_3 - x_1}} \Pi \left( \phi, \frac{x_2 - x_1}{-x_1}, \sqrt{\frac{x_2 - x_1}{x_3 - x_1}} \right) \right) \times \\ &\quad \left( x_1 + (x_2 - x_1) \text{sn}^2 \left( \frac{\sqrt{x_3 - x_1}}{2} s, \sqrt{\frac{x_2 - x_1}{x_3 - x_1}} \right) \right),\end{aligned}$$

where  $\phi = \text{am} \left( \frac{\sqrt{x_3 - x_1}}{2} s, \sqrt{\frac{x_2 - x_1}{x_3 - x_1}} \right)$ , and  $\text{am}$  denotes the jacobi amplitude function.

**Proposition 4.19.** *If the solitons rotate around the  $z$ -axis, then  $\psi$  is unbounded and its infimum is 0.*

*Proof.* By applying the rotation matrix given in (4.6), after  $n$  cycles, points  $(\psi, \psi \cos \theta, \psi \sin \theta)$  in the first cycle are rotated to the points

$$\left( \cosh(n\omega) + \sinh(n\omega) \cos \theta, \sinh(n\omega) + \cosh(n\omega) \cos \theta, \sin \theta \right) \psi.$$

To analyze the behavior of  $\psi$ , we consider specific values of  $\theta$ . For  $\theta_0 = \pi$ ,  $\psi_n = \exp(-n\omega)\psi_0$ , where  $\psi_0$  is the value of  $\psi$  at  $\theta = \theta_0$  in the first period. As  $n \rightarrow +\infty$ ,  $\psi_n \rightarrow 0$ . For  $\theta_0 = 2\pi$ ,  $\psi_n = \exp(n\omega)\psi_0$ , where again  $\psi_0$  is the value of  $\psi$  at  $\theta = \theta_0$  in the first period. As  $n \rightarrow +\infty$ ,  $\psi_n \rightarrow +\infty$ . Thus, we have shown that  $\psi$  is unbounded and its infimum is 0, as desired.  $\square$

Given the initial condition  $\theta(0) = \frac{\pi}{2}$ , and following the preceding proof, we arrive at the subsequent expressions

$$\sin \theta(nT) = \frac{1}{\cosh(n\omega)}, \quad \cos \theta(nT) = \frac{\sinh(n\omega)}{\cosh(n\omega)}.$$

From these derived expressions, we formulate the following corollary.

**Corollary 4.20.** *When solitons rotate around the  $z$ -axis with the initial condition  $\theta(0) = \frac{\pi}{2}$ , it holds that  $2n\pi < \theta(nT) < \frac{(4n+1)\pi}{2}$ . The angle  $\theta(nT) - 2n\pi$  decreases monotonically as  $n$  increases, and as the integer  $n$  approaches positive infinity,  $\theta(nT) - 2n\pi$  converges to zero.*

**Remark 4.21.** With the initial conditions  $\psi(0) = \frac{-x_1}{\sqrt{-\mu}}$  and  $\psi_s(0) = 0$ , our numerical calculations (depicted in the right-hand side of Fig. 4) reveal that  $\theta(T, \lambda)$  exhibits a monotonically increasing behavior with respect to  $\lambda$ . Additionally, we observe the following asymptotic behavior:  $\theta(T, \lambda) \rightarrow 2\pi$  as  $\lambda \rightarrow 3(\mu/2)^{2/3}$ , and  $\theta(T, \lambda) \rightarrow \frac{5\pi}{2}$  as  $\lambda \rightarrow +\infty$ .

**4.4. Proof of Theorem 1.4.** Based on previous insights, we have developed a method for solving the differential equation (1.5).

*Proof of Theorem 1.4.* Through meticulous computation, we verify that

$$2ff_{ss} - f_s^2 - 2f^3 = x_1x_2x_3.$$

Following the guidance provided by previous hints, we postulate that the solution can be formulated as

$$\psi(s) = f(s)G(\theta),$$

and  $\theta$  is defined through the differential relationship  $\frac{d\theta}{ds} = \frac{1}{\psi}$ . Consequently, this second-order differential equation can be rewritten as

$$G_{\theta\theta} - \frac{3G_{\theta}^2}{2G} - \frac{G}{2} + \frac{G^3}{2}x_1x_2x_3 = 0.$$

Utilizing Proposition 2.1, we are able to draw the desired conclusions.  $\square$

**Data availability** No data availability statement is required, as no experimental data is involved.

**Conflict of interest** The authors have no conflict of interest to declare that are relevant to the content of this article.

## REFERENCES

- [Abresch and Langer 1986] U. ABRESCH, J. LANGER, The normalized curve shorting flow and homothetic solution. *J. Differential Geom.*, **23** (1986), 175–196.
- [Andrews 1994] B. ANDREWS, Harnack inequalities for evolving hypersurfaces, *Math. Z.*, **217** (1994), 179–197.

- [Andrews and Baker 2004] B. ANDREWS, C. BAKER, A comparison of self-similar solutions of mean curvature flow and Ricci flow, *J. Differential Geom.*, **67**(1), 1–31, 2004.
- [Angenent et al. 1998] S. ANGENENT, G. SAPIRO, A. TANNENBAUM, On the affine heat equation for nonconvex curves, *J. Amer. Math. Soc.*, **11** (1998), 601–634.
- [Benci and Fortunato 1994] V. BENCI, D. FORTUNATO, On the existence of infinitely many geodesics on space-time manifolds. *Adv. Math.*, **105** (1994), 1–25.
- [Birkhoff 1927] G. D. BIRKHOFF, *Dynamical Systems*, American Mathematical Society, 1927.
- [Brakke 1978] K. A. BRAKKE, *The Motion of a Surface by Its Mean Curvature*, Princeton University Press, 1978.
- [Bryan et al. 2020] M. N. BRYAN, M. IVAKI, J. SCHEUER Harnack inequalities for curvature flows in Riemannian and Lorentzian manifolds, *J. Reine Angew. Math.*, **764** (2020), 71–109.
- [Byard and Friedman 1971] P. F. BYARD, M. D. FRIEDMAN, *Handbook of Elliptic Integrals for Engineers and Scientists*, 2nd Edition, Springer-Verlag, Berlin, 1971.
- [Chow 1991] B. CHOW, On Harnack’s inequality and entropy for the Gaussian curvature flow, *Commun. Pure Appl. Math.*, **44** (1991), no. 4, 469–483.
- [Colding and Minicozzi 2003] T. H. COLDING, W. P. MINICOZZI, *Generic mean curvature flow in higher dimensions*, *Ann. of Math.*, **167**(2), 833–888, 2003.
- [Duggal and Bejancu 1996] K. L. DUGGAL, A. BEJANCU, *Lightlike Submanifolds of Semi-Riemannian Manifolds and Applications*, Kluwer Academic, Dordrecht, 1996.
- [Einstein 1905] A. EINSTEIN, Zur Elektrodynamik bewegter Körper, *Ann. Phys.*, **332**(1905), 891–921.
- [Evans and Spruck 1991] L. C. EVANS and J. SPRUCK, Motion of level sets by mean curvature, *J. Differential Geom.*, **33**(3), 635–681, 1991.
- [Gardner et al. 1967] C. S. GARDNER, J. M. GREENE, M. D. KRUSKAL, R. M. MIURA, *Method for Solving the Korteweg-de Vries Equation*, *Phys. Rev. Lett.*, **19**, 1095–1097, 1967.
- [Gage 1983] M. GAGE, *An Isoperimetric Inequality with Application to Curve Shortening*, *Duke Math. J.*, **50** (1983), 1225–1229.
- [Gage 1984] M. GAGE, *Curve Shortening Makes Convex Curves Circular*, *Invent. Math.*, **76** (1984), 357–364.
- [Gage and Hamilton 1986] M. GAGE, R. HAMILTON, *The Heat Equation Shrinking Convex Plane Curves*, *J. Differential Geometry*, **23** (1986), 69–96.
- [Gradshteyn and Ryzhik 2014] S. GRADSHTEYN, I. M. RYZHIK, *Table of Integrals, Series, and Products*, Daniel. Zwillinger and Victor Moll, (eds.), 2014.
- [Hamilton 1982] R. S. HAMILTON, Three-manifolds with positive Ricci curvature, *J. Differential Geom.*, **17**(2), 255–306, 1982.
- [Hamilton 1989] R. S. HAMILTON, *Lecture Notes on Heat Equation in Geometry*, Honolulu, Hawaii, 1989.
- [Hamilton 1993] R. S. HAMILTON, The Harnack estimate for the Ricci Flow, *J. Differential Geom.*, **37** (1993), 225–243.
- [Hamilton 1995a] R. S. HAMILTON, Harnack estimate for the mean curvature flow, *J. Differential Geom.*, **41** (1995), 215–226.
- [Hamilton 1995b] R. S. HAMILTON, The formation of singularities in the Ricci flow, *Surv. Differential Geom.*, **2**, 1–136, 1995.
- [Hawking 1965] S.W. HAWKING, *Occurrence of singularities in open universes*, *Phys. Rev. Lett.*, **15** (1965), 689–690.
- [Hawking 1966a] S.W. HAWKING, *The occurrence of singularities in cosmology*, *Proc. Roy. Soc. (London) A*, **294** (1966), 511–521.

- [Hawking 1966b] S.W. HAWKING, *The occurrence of singularities in cosmology II*, *Proc. Roy. Soc. (London) A*, **295** (1966), 490–493.
- [Hawking 1967] S.W. HAWKING, *The occurrence of singularities in cosmology III. Causality and singularities*, *Proc. Roy. Soc. (London) A*, **300** (1967), 187–201.
- [Hawking and Ellis 1973] S. W. HAWKING, G. F. R. ELLIS, *The Large Scale Structure of Space-Time*, Cambridge University Press, 1973.
- [Huiskens 1990] G. HUISKEN, Asymptotic behavior for singularities of the mean curvature flow. *J. Differential Geom.*, **31** (1990), 285–299.
- [Huiskens 1993] G. HUISKEN, *Local and global behavior of hypersurfaces moving by mean curvature*. Differential geometry: partial differential equations on manifolds (Los Angeles, CA, 1990), Proc. Sympos. Pure Math., vol. 54, Amer. Math. Soc., Providence, RI, 1993, pp. 175–191.
- [Hungerbühler and Smoczyk 2000] N. HUNGERBUHLER, K. SMOCZYK, Soliton solutions for the mean curvature flow. *Diff. Int. Eq.*, **13** (2000), 1321–1345.
- [Jiang et al. 2023] X. JIANG, Y. YANG, Y. YU, An eternal curve flow in centro-affine geometry, *J. Funct. Anal.*, **284**(10) (2023), 109904.
- [Kovalev 2015] A. B. KOVALEV, *Introduction to Nonlinear Dynamics and Chaos*, Wiley, 2015.
- [Li and Yau 1986] P. LI, S.-T. YAU, On the parabolic kernel of the Schrödinger operator, *Acta Math.*, **156**, 153–201, 1986.
- [Liu 2004] H. LIU, Curves in the lightlike cone, *Beitr. Algebra Geom.*, **45** (2004), 291–303.
- [Lima and Montenegro 1999] L. LOPEZ DE LIMA, J. F. MONTENEGRO, Classification of solitons for the affine curvature flow. *Commun. Anal. Geom.*, **4** (1999), 731–753.
- [Minkowski 1908] H. MINKOWSKI, *Minkowski Space and Time*, Proceedings of the Cologne Conference, 1908.
- [Misner et al. 1973] C. W. MISNER, K. S. THORNE, J. A. WHEELER, *Gravitation*, W. H. Freeman, 1973.
- [Nakahara 2003] M. NAKAHARA, *Geometry, Topology and Physics*, Institute of Physics Publishing, 2003.
- [Niu and Yang 2025] H. NIU AND Y. YANG, The soliton solutions of a third-order centro-affine curvature flow, *Math. Ann.*, (2025), online.
- [O’Neill 1983] B. O’NEILL, *Semi-Riemannian Geometry: With Applications to Relativity*, Academic Press, 1983.
- [Olver 2008] P. J. OLVER, Invariant submanifold flows. *J. Phys. A: Math. Theor.*, **41** (2008), 344017.
- [Olver et al. 2020] P.J. OLVER, C.Z. QU, Y. YANG, Feature matching and heat flow in centro-affine geometry, *Symmetry Integrability Geom. Methods Appl.*, **16** (2020), 093.
- [Parikh and Svesko 2018] M. PARIKH, A. SVESKO, Einstein’s equations from the stretched future light cone. *Phys. Rev. D*, **98** (2018), 026018.
- [Penrose 1965] R. PENROSE, Gravitational Collapse and Space-Time Singularities, *Phys. Rev. Lett.*, **14**, 57–59, 1965.
- [Penrose 2020] R. PENROSE, *Black Holes, Cosmology and Space-Time Singularities*, Nobel Lecture, December 8, 2020, University of Oxford, Oxford, United Kingdom.
- [Perelman 2002] G. PERELMAN, *The entropy formula for the Ricci flow and its geometric applications*, arXiv:math/0211159, 2002.
- [Poincaré 1892] H. POINCARÉ, *Les Méthodes Nouvelles de la Mécanique Céleste*, Gauthier-Villars, 1892.

- [Press et al. 2007] W. H. PRESS, S. A. TEUKOLSKY, W. T. VETTERLING, B. P. FLANNERY, *Numerical Recipes: The Art of Scientific Computing (3rd ed.)*, Cambridge University Press, 2007.
- [Rindler 2001] W. RINDLER, *Introduction to Special Relativity*, Oxford University Press, 2001.
- [Sachs and Wu 1977] R. K. SACHS, H. WU, *General Relativity for Mathematicians*, Springer-Verlag, 1977.
- [Sapiro and Tannenbaum 1994] G. SAPIRO, A. TANNENBAUM, On affine plane curve evolution, *J. Funct. Anal.*, **119** (1994), 79–120.
- [Silva and Tenenblat 2023] F. N. DA SILVA AND K. TENENBLAT, Self-similar solutions to the curvature flow and its inverse on the 2-dimensional light-cone, *Ann. Mat. Pura Appl.*, **202** (2023), 253–285.
- [Strogatz 1994] S. H. STROGATZ, *Nonlinear Dynamics and Chaos: With Applications to Physics, Biology, Chemistry, and Engineering*, Addison-Wesley, 1994.
- [Vrăncăanu and Roșca 1976] G. VRĂNCEANU, R. ROȘCA, *Introduction to Relativity and Pseudo-Riemannian Geometry*, Editura Academiei Republicii Socialiste România, 1976.
- [Walrave 1995] J. WALRAVE, *Curves and surfaces in Minkowski space*, Thesis (Ph.D.), Katholieke Universiteit. Leuven (Belgium), 1995.
- [Yang 2023] Y. YANG, The maximal curves and heat flow in general-affine geometry. *Differential Geom. Appl.*, **91** (2023), 102079.
- [Zabusky and Kruskal 1965] N. J. ZABUSKY, M. D. KRUSKAL, Interaction of “Solitons” in a Collisionless Plasma and the Recurrence of Initial States, *Phys. Rev. Lett.*, **15**, 240–243, 1965.

YUN YANG

DEPARTMENT OF MATHEMATICS, NORTHEASTERN UNIVERSITY, SHENYANG, 110819,  
P.R. CHINA

*Email address:* yangyun@mail.neu.edu.cn